HHS Public Access

Author manuscript

Exp Eye Res. Author manuscript; available in PMC 2019 October 01.

Published in final edited form as:

Exp Eye Res. 2018 October ; 175: 192–198. doi:10.1016/j.exer.2018.06.015.

Chemical chaperone treatment improves levels and distributions of connexins in Cx50D47A mouse lenses

Oscar Jara, **Peter J. Minogue**, **Viviana M. Berthoud**, and **Eric C. Beyer**

Department of Pediatrics, University of Chicago, Chicago, Illinois

Abstract

Mouse Cx50D47A and human Cx50D47N are non-functional connexin mutants that cause dominantly-inherited cataracts. In tissue culture expression experiments, they both exhibit impaired cellular trafficking and gap junction plaque formation. Lenses of mice expressing Cx50D47A have cataracts, reduced size, drastically decreased levels of connexin50, and less severely reduced levels of connexin46. The PERK-dependent pathway of the ER response to misfolded proteins is activated, and they have impaired differentiation with retained cellular organelles. Since treatments that enhance protein folding improve trafficking and plaque formation by Cx50D47N and other mutant connexins *in vitro*, and they are successful therapeutics for some other diseases caused by misfolded proteins, we tested the efficacy of the chemical chaperone, 4-phenylbutyrate (4-PBA) in cultured cells and mice expressing Cx50D47A. 4-PBA treatment increased the formation of Cx50D47A-containing plaques at appositional membranes of transiently transfected HeLa cells. Heterozygous Cx50D47A mice were treated with 4-PBA by addition to the drinking water and parenteral injection of pregnant mice (starting 10 days after pairing of males and females) and their pups. Lenses from l-month-old mice were examined by darkfield illumination and immunofluorescence microscopy. Protein levels were determined by immunoblotting. Cataract size and density were not detectably different between the control and the 4-PBA-treated groups. Lens size was not increased following treatment. Levels of connexin46 and connexin50 were significantly increased in 4-PBA-treated lenses compared with saline-treated lenses. Immunofluorescence showed an increased abundance of connexin46 immunoreactivity and puncta. The ratio of phosphorylated to total EIF2α was not altered, and levels of organellar proteins were not significantly reduced, suggesting that the ER response to misfolded proteins and differentiation were not changed. Thus, treatment with 4-PBA improved critical pathological issues in these mice (low connexin and gap junction abundance), but the magnitude of this recovery (especially for Cx50) was inadequate to impact the reduced size or the opacification of Cx50D47A lenses.

Address correspondence to: Eric C. Beyer MD PhD, Department of Pediatrics University of Chicago, 900 East 57th St., KCBD-5152, Chicago, IL 60637, Telephone: (773) 834-1498, FAX: (773) 834-1329, ecbeyer@uchicago.edu.

1. Introduction

Cataracts are opacifications of the lens that disrupt the normal transmission and focusing of light. Congenital cataracts are the most common treatable cause of childhood blindness with an incidence of ~2/10,000 births (reviewed in Reddy, 2004). Elucidating the pathophysiology of genetically-determined congenital cataracts may help in understanding the causes of other cataracts and may facilitate the development of preventative or therapeutic approaches.

Congenital cataracts can be caused by mutations of a number of genes expressed in the lens, including those that encode structural proteins and transcription factors (summarized in http://cat-map.wustl.edu/) (Shiels et al., 2010). A large number of different missense and frame-shift mutations of the lens connexins, connexin46 (Cx46) and connexin50 (Cx50), have been identified in families with inherited cataracts (reviewed in Beyer et al., 2013). These two proteins form gap junctions that facilitate intercellular communication between lens fiber cells. Nearly all of the connexin mutant-linked cataracts are inherited as autosomal dominant traits.

Our laboratory has been interested in determining the biochemical, cell biological and physiological abnormalities of the lens connexin mutants. Studies of mutants using expression systems have shown that many cataract-associated connexin mutants form few or no gap junction plaques and do not support significant intercellular communication (Beyer et al., 2013). Often, the mutant connexin localizes within compartments of the protein biosynthetic/secretory pathway (e.g., the ER, ERGIC, and/or Golgi apparatus), suggesting that the protein has been retained within the export pathway due to misfolding and/or incomplete/improper oligomerization. Representative cataract-associated connexin mutants that exhibit these behaviors *in vitro* include the Cx50 mutants with aspartate-47 substitutions, mouse Cx50D47A and human Cx50D47N (Steele et al., 1998; Xu and Ebihara, 1999; Arora et al., 2008). In *Xenopus* oocyte expression studies, these mutants do not form functional gap junction channels; however, they do not act as dominant-negative inhibitors of co-expressed wild type Cx50 (Xu and Ebihara, 1999; Arora et al., 2008).

We have extensively characterized the abnormalities caused by expression of Cx50D47A in mice. These animals have lenses that are smaller than those of wild type littermates and contain cataracts (Berthoud et al., 2013). Levels of Cx50 are decreased to near zero, and Cx46 levels are also reduced (although less severely). In the lens, it is likely that the mutant associates with its wild type Cx50 counterpart and the co-expressed Cx46, leading to their retention in the cytoplasm and degradation (Berthoud et al., 2013). The lenses of Cx50D47A mice show persistence of nuclear remnants in deep regions of the lens and elevated levels of nuclear, mitochondrial, and some ER proteins (Berthoud et al., 2013, 2016). Lenses of Cx50D47A mice show activation of the PERK/EIF2a-dependent pathway of the ER response to misfolded proteins (Berthoud et al., 2016).

Some other diseases caused by mutations of secreted or membrane proteins that are misfolded and retained within cytoplasmic biosynthetic compartments have been treated with a group of small molecules called chemical chaperones. These agents may facilitate

folding of the mutant protein, restoring function and reducing ER stress (Mu et al., 2008). 4-Phenylbutyrate (4-PBA) is one of the most commonly utilized chemical chaperones (reviewed in Kolb et al., 2015). It is the active component of sodium phenylbutyrate which is approved for treatment of urea cycle disorders (Batshaw et al., 2001). Its pharmacological properties have been extensively studied: it is water-soluble, orally bioavailable, and has good penetration into the central nervous system and across the placenta. It has been successfully used in mice to treat a variety of different diseases involving protein misfolding or ER stress (Basseri et al., 2009;Koyama et al., 2014;Yokoi et al., 2015;Lee et al., 2017).

Previous studies suggested that some misfolded Cx50 mutants might be susceptible to rescue of their protein trafficking. Culture of cells expressing human Cx50D47N at reduced temperatures (a more permissive condition for protein folding) facilitates formation of gap junction plaques in transfected cells. In addition, 4-PBA treatment of cultured cells expressing a different Cx50 mutant (Cx50P88S) rescues the formation of gap junction structures (Berthoud et al., 2003). Therefore, we hypothesized that 4-PBA treatment might improve folding of Cx50D47A and rescue its plasma membrane trafficking; this could decrease degradation of co-expressed wild-type Cx50 and Cx46. We tested the effects of 4-PBA on Cx50D47A expressed in transfected cells. We also used the drug to treat heterozygous Cx50D47A mice (which mimic the situation in people with autosomal dominant congenital cataracts) to test whether it would improve levels of wild-type connexins (Cx50 and Cx46), improve lens growth, and ameliorate cataract formation.

2. Methods

2.1. Chemicals

Pharmaceutical grade 4-PBA was obtained from Scandinavian Formulas (Sellersville, PA). All other chemicals were obtained from Sigma Chemical Co. (St. Louis, MO, USA) unless otherwise specified.

2.2. Cell culture and transfection

HeLa cells were cultured and transfected with pcDNA3.1 plasmid encoding mouse Cx50D47A as previously described (Arora et al., 2008). Twenty four hours after transfection the cultures were treated with 5 mM 4-PBA (or left untreated) for an additional 24 hrs. Then, they were fixed in 4% paraformaldehyde, and Cx50 was localized by immunofluorescence (Berthoud et al., 2003). Specimens were studied in an Axioplan 2 microscope (Carl Zeiss, Munchen, Germany) equipped with a mercury lamp. Images were acquired with a Zeiss AxioCam digital camera using Zeiss AxioVision software.

2.3. Animals

Cx50D47A (No2, ENU-326) mice (originally identified by Favor (1983) by screening for the cataract phenotype following ethylnitrosourea mutagenesis) were maintained in the C3H mouse strain as described previously (Berthoud et al., 2013). All animal procedures followed the University of Chicago Animal Care and Use Committee guidelines.

2.4. 4-PBA treatment of animals

Treatment began 10 days after pairing of males and females. The pregnant mice were allowed to drink water or water containing 60 mM 4-PBA *ad libitum*. Some mice were given larger doses of 4-PBA in their drinking water (as described in Results). In other experiments, pregnant mothers received injections of 4-PBA (in saline; 400 mg/kg) in addition to water containing 60 mM 4-PBA. After birth, the pups were injected with 4-PBA (400 mg/kg), and the mother was allowed to drink 4-PBA-containing water. After weaning, pups received 4-PBA in the drinking water and by injection. The drug was given intraperitoneally in all mice, except for a few days following birth when it was given subcutaneously. Control animals received injections of an equal volume of saline besides *ad libitum* access to drinking water. Water was changed daily for all animals. Body weights did not differ between controls and the animals that received 60 mM 4-PBA in their drinking water (with or without parenteral injection of the drug).

2.5. Light microscopy analysis of whole lenses

Darkfield photomicrographs of lenses were obtained using a Zeiss Stemi-2000C dissecting scope and a Zeiss AxioCam digital camera using Zeiss AxioVision software. All lenses were photographed using the same magnification, illumination and exposure times. Cataracts (opacities) were quantified in photomicrographs using NIH ImageJ software (https://imagej.nih.gov/ij/) by an investigator who was unaware of the treatment status of the lenses. The cataract was encompassed within a circle, the size of which was chosen to enclose the largest cataract found in all experimental animals (Fig. 1). A circle of identical size was used for analysis of all images. The gray values within the area delimited by the circle were determined and integrated using NIH ImageJ. These data (mean gray value x area) are reported in arbitrary units. The sizes of lenses were determined from the photomicrographs by measuring the major and minor diameters using NIH ImageJ software.

2.6. Antibodies

Rabbit polyclonal anti-human Cx50 and anti-mouse Cx46 antibodies have been previously described (Berthoud et al., 2003, 2013). Rabbit monoclonal anti-EIF2α (D7D3) (catalog # 5324P; lot 3; RRID:AB_11178937), anti-P-EIF2α (Ser-51) (D9G8) (catalog # 3398P; lot 2; RRID:AB_2096481), anti-H3 histone (D1H2) (catalog #4499S; RRID:AB_10544537), and anti-calreticulin (D3E6) (catalog #12238S; RRID:AB_2688013) antibodies were obtained from Cell Signaling Technology (Danvers, MA, USA). Rabbit polyclonal anti-Tom20 antibodies (FL-145 (catalog # sc-11415; RRID:AB_2207533) were obtained from Santa Cruz Biotechnology (Santa Cruz, CA). Alexa Fluor® 488 goat anti-rabbit IgG antibodies (catalog # A-11034, RRID:AB_2576217) were obtained from Thermo Fisher Scientific (Waltham, MA, USA). HRP-conjugated goat anti-rabbit antibodies (catalog # 115-036-072, RRID:AB_2338525) were obtained from Jackson ImmunoResearch (West Grove, PA, USA).

2.7. Immunoblotting

Lenses were dissected in phosphate buffered saline pH 7.4 (PBS), homogenized in PBS containing 20 mM NaF and 10 mM sodium orthovanadate to inhibit phosphatases, and 2

mM PMSF and cOmplete EDTA-free protease inhibitor cocktail (Roche Applied Science, Indianapolis, IN, USA) to inhibit protease activity in a glass-glass homogenizer, and then sonicated. Homogenates were stored at −80°C until used. Protein concentrations were determined using the BioRad Protein Assay (BioRad, Hercules, CA, USA) based on the Bradford dye-binding procedure (Bradford, 1976). Immunoblots were performed as described in Minogue et al. (2009) and Berthoud et al. (2016) after loading aliquots from lens homogenates containing equal amounts of total protein. Immunoblots were performed in at least 3 independent experiments and quantified by densitometry using Adobe Photoshop (Adobe Systems Incorporated, San Jose, CA, USA).

2.8. Immunofluorescence microscopy of lens sections

Lenses from 1 month-old mice were fixed for 1 hour in 4% paraformaldehyde in PBS. The lenses were rinsed 3 × 15 minutes in PBS. Then, they were transferred to 30% sucrose in PBS and left at 4°C until they sank. Cryostat sections (20 μm) were obtained and then processed for immunofluorescence with anti-Cx46 or anti-Cx50 antibodies, followed by incubation with Alexa Fluor 488 goat anti-rabbit IgG antibodies, TRITC-conjugated phalloidin (Sigma) to stain filamentous actin and with DAPI (Invitrogen, Carlsbad, CA, USA) to stain nuclei as previously described (Berthoud et al., 2013).

Confocal images were obtained using a Leica SP8 laser scanning confocal microscope using the factory settings for excitation and emission wavelengths of Alexa Fluor® 488, TRITC or DAPI fluorescence. Images were collected by sequential scanning using single laser-line excitation to eliminate bleeding between channels.

Figures were assembled using Adobe Photoshop CC. Fluorescent signals were analyzed using NIH ImageJ software. All images were analyzed in two ways: (1) The mean gray value was determined in a region of interest that encompassed epithelium and superficial underlying fiber cells (delimited area 1 in Fig. 2) or that contained a substantial bulk of more interior fiber cells (enclosed area 2 in Fig. 2); (2) The number of particles (>2 pixels) above a threshold (to exclude background staining) was counted in a region of interest within fiber cells (Fig. 2, area 2).

3. Results

3.1. 4-PBA treatment improved Cx50D47A trafficking in HeLa cells

As an initial screen of whether 4-PBA treatment might improve cellular trafficking and gap junction formation by Cx50D47A, HeLa cells were transiently transfected with the mutant connexin and then left untreated or treated with 4-PBA. Immunofluorescent staining showed that Cx50D47A localized within the cytoplasm in a reticular and perinuclear distribution (Fig. 3, left panel) as previously reported (Arora et al., 2008), implying that the protein is retained in the biosynthetic/secretory pathway. Treatment of Cx50D47A-transfected cells with 4-PBA resulted in some bright, punctate staining at appositional membranes consistent with the formation of gap junction plaques (Fig. 3, right panel).

3.2. Treatment of mice with 4-PBA had little effect on cataracts or lens size

We next sought to test whether 4-PBA would affect the pathologic lens phenotypes of mice carrying the Cx50D47A mutation. We initially treated heterozygous Cx50D47A mice by addition of 4-PBA to the drinking water at a final concentration of 60 mM, since this dose was well tolerated and efficacious in previous studies of diseases of other tissues (Basseri et al., 2009;Kemter et al., 2014;Lee et al., 2017). We examined the lenses of treated and control mice at 1 month of age by darkfield microscopy. Lenses from control, heterozygous Cx50D47A mice had cataracts at this age (Fig. 4A, left panel), as previously reported (Berthoud et al., 2013). In 4-PBA-treated mice, the lenses showed variability in their appearances; some were nearly transparent, while others had cataracts that appeared as severe as those of control animals (Fig. 4A, right panels). The cataracts of 4-PBA-treated mice (quantified as the integrated gray value in an area containing the opacity) were not significantly different from those of control mice (Fig. 4B) . Because Cx50D47A expression reduces lens growth, we determined the major and minor diameters of the lenses of untreated and treated mice. There were no differences in the major or minor diameters of these lenses (Fig. 5A).

Because 4-PBA is readily bio-available, we tried increasing the concentration of the drug in the drinking water. Pregnant mice that were allowed to drink water containing 80 mM 4-PBA had normal litter sizes, but their offspring suffered from stunted growth compared to the controls. Pregnant mice given water containing 120 mM 4-PBA, either did not maintain pregnancies or had small litters of feeble mice that did not gain weight. At these higher concentrations, water intake was greatly decreased and might have accounted for some or all of the negative effects.

We then tried adding parenteral injections of 4-PBA (400 mg/kg) to the mice given 60 mM 4-PBA in their drinking water. Lens appearance and size were assessed in control and treated mice at 1 month of age. Darkfield micrographs showed that lenses of control mice and those treated with injections and oral 4-PBA both had opacities of variable sizes and densities (Fig. 4C). Quantification of these opacities showed no significant differences between treated and control mice (Fig. 4D). We also measured the major and minor diameters of these lenses to assess lens sizes. Treatment did not produce an increase in lens size; both the major and minor diameters of the 4-PBA-treated (water + injection) mice were slightly (but significantly) smaller than those of the controls (Fig. 5B).

3.3. Treatment of mice with 4-PBA increased fiber cell connexins

Because reductions of lens fiber connexins and gap junctions are central to the pathogenesis of the lens abnormalities caused by expression of Cx50D47A, we assessed the levels and distributions of Cx50 and Cx46 in control mice and mice that received 4-PBA (both in their drinking water and via parenteral injection). Immunoblots of lens homogenates from 1-month-old mice showed that treatment with 4-PBA led to significant increases in the levels of both Cx50 and Cx46 (Fig. 6). Cx50 levels were increased by 44%, and Cx46 levels were increased by 62%.

We assessed the distributions of the fiber cell connexins by immunofluorescent staining of sections from lenses of 1-month-old mice (Fig. 7). The distribution of Cx50 immunoreactivity in treated animals appeared similar to that of controls (Fig. 7A). No significant differences were found between control and 4-PBA-treated lenses in Cx50 immunoreactivity mean gray value in surface or fiber cells regions or in the number of Cx50 immunoreactive particles within fiber cell regions (Fig. 7B and C). In contrast, Cx46 immunoreactivity appeared very different. Control lenses had only rare spots of Cx46 staining that were mostly located between fiber cells; however, lens sections from a 4-PBA-treated mouse showed many more puncta of Cx46 immunoreactivity between fiber cells (Fig. 7D). Quantification of immunoreactive Cx46 showed significant increases in average gray values (within surface and fiber cell regions) and in immunoreactive particles that likely represent Cx46-containing gap junctions (Fig. 7E and F).

3.4. Treatment with 4-PBA did not affect the activation of the PERK/EIF2α pathway in Cx50D47A lenses

Because the PERK/EIF2α transducing pathway is activated in Cx50D47A lenses (Berthoud et al., 2013), we assessed whether 4-PBA treatment had an effect on its activation. For this purpose, we examined the levels of phosphorylated EIF2α and total EIF2α in lenses of 1-month-old control and 4-PBA-treated mice (Fig. 8A and B). We found no significant difference in the levels of phosphorylated EIF2α and total EIF2α (Fig. 8A and B), or in the ratio of phosphorylated to total EIF2a (Fig. 8C).

3.5. Treatment with 4-PBA did not affect levels of organelle proteins in Cx50D47A lenses

Cx50D47A lenses have abnormalities of differentiation including impaired degradation of cellular organelles (Berthoud et al., 2013). This leads to increases of marker proteins for nuclei (histone 3) and mitochondria (Tom20) (Berthoud et al., 2013). These lenses also have greater levels of some (but not all) proteins that are abundant within the ER (like calreticulin) (Berthoud et al., 2016). We used immunoblotting to examine the levels of these proteins in lenses of 1-month-old control and 4-PBA-treated mice (Fig. 9A-C). Although average levels of each of these proteins decreased, the differences did not reach statistical significance ($p > 0.05$ for all three proteins) .

4. Discussion

4-PBA is a chemical chaperone that has improved the cellular trafficking of a variety of different mutant membrane or secreted proteins in tissue culture systems (Rubenstein et al., 1997;Cheong et al., 2006;Hayashi and Sugiyama, 2007). We found that 4-PBA treatment improved the trafficking of Cx50D47A such that it formed gap junction plaques in transfected HeLa cells. Treatment with 4-PBA also improves the formation of gap junction plaques by a different Cx50 mutant, Cx50P88S, which forms aggregates in transfected cells (Berthoud et al., 2003). The 4-PBA effects on these mutants are likely achieved by improving protein folding and minimizing degradation or aggregation (Upagupta et al., 2017).

Based on this *in vitro* result, we hypothesized that 4-PBA might have some efficacy *in vivo*: better trafficking of the non-functional (but non-inhibitory) mutant Cx50D47A, might decrease the cytoplasmic retention and degradation of wild type lens connexins that associate with the mutant. We found that treatment with 4-PBA improved levels of both Cx46 and Cx50 and the abundance/distribution of Cx46 gap junction plaques in Cx50D47A heterozygous lenses. The 62% increase in levels of Cx46 represents a major increase in the abundance of Cx46 in the lens fiber cells, although probably not a complete return to 100%, since untreated heterozygous lenses have ~61% of wild type levels (Berthoud et al., 2013). However, because Cx50 levels are very low in Cx50D47A heterozygotes (~10% of wild type) (Berthoud et al., 2013), the 4-PBA-induced increase would only bring its levels to ~14% of the Cx50 levels in a wild type mouse lens and would include both wild type and mutant protein. Because the mutant allele is nonfunctional (Xu and Ebihara, 1999), the significant improvement of Cx50 levels would only produce a small absolute amount of functional Cx50. Thus, the amount of functional Cx50 needed for normal transparency and lens growth must be somewhere between this value and 50%, since heterozygous Cx50-null mice have transparent lenses of normal size (White et al., 1998).

Treatment with 4-PBA has previously proven effective in ameliorating clinical aspects of several different diseases such as familial epilepsy and RYR1 myopathy in mouse models, (Yokoi et al., 2015;Lee et al., 2017). However, similar to the lack of significant improvement in lens transparency and size in Cx50D47A mice, 4-PBA treatment did not ameliorate the clinical attributes of some other diseases caused by misfolded proteins in mice or humans including a1-antitrypsin deficiency and uromodulin-associated kidney disease (Teckman, 2004;Kemter et al., 2014). It is possible that the critical requirement is not just improved protein folding, but relief of ER stress. This suggestion is supported by the observations that 4-PBA has been effective for some diseases involving multiple aspects of ER stress and the unfolded protein response (Basseri et al., 2009;Koyama et al., 2014). In contrast, we observed no reduction of the ER response to misfolded protein in Cx50D47A lenses (i.e. P-EIF2α/EIF2α was not affected by 4-PBA treatment).

Although we did not specifically assess 4-PBA levels in the lens, it is unlikely that delivery of the drug was inadequate. Excellent serum levels are achieved even after mice are given smaller doses (Yokoi et al., 2015). We gave the drug both orally and parenterally, even though the drug is orally bioavailable. Because the drug has a relatively short half-life in the body, we made it continuously available through the drinking water. In addition, drug treatment was started at the approximate time when lens development begins and continued until 1 month of age. Although the lens would be avascular at the end of our treatment period, the lenses of these mice would have had a hyaloid vasculature for much of the time (i.e. from its development until its regression around post-natal day 12–15). The improvements in Cx46 and Cx50 levels and of Cx46 gap junction particles in the 4-PBA-treated heterozygous lenses support our contention that 4-PBA reached the lens.

Does pharmacological treatment of cataracts require specificity for the misfolded protein? As a chemical chaperone, the 4-PBA treatment is not specific for misfolded connexins. 4-PBA has previously been shown to improve the solubility of a mutant γ-crystallin and the apoptosis that it causes in cultured lens epithelial cells (Gong et al., 2010), but it is unknown

if it would have any efficacy for this mutant *in vivo*. Recently, several sterols have been shown to disaggregate crystallin aggregates *in vitro* and to ameliorate (but not produce complete resolution of) cataracts *in vivo* (Makley et al., 2015;Zhao et al., 2015). However, in an *ex vivo* study, lanosterol treatment produced no improvement or was accompanied by progression of human age-related cataracts (Shanmugam et al., 2015), raising some controversies about the benefits of sterol treatment.

The changes in lens connexin levels and increased Cx46 gap junction formation might not have resulted only from improved protein folding due to the chaperone function of 4-PBA. This drug has other pharmacological effects. 4-PBA has been used many times as an inhibitor of histone deacetylases (HDAC). In other cell types, 4-PBA increased intercellular communication mediated by connexin43 (Cx43) (Ammerpohl et al., 2004;Khan et al., 2007;Wang et al., 2015). While HDAC inhibition was invoked as a mechanism in these reports, increases in Cx43 mRNA were not consistently observed. In addition, 4-PBA can have more general influences on autophagy and other aspects of proteostasis by altering gene expression (Lam et al., 2013).

In summary, 4-PBA treatment at tolerated doses was insufficient to produce significant improvements in the major pathologies of Cx50D47A lenses: opacification and growth reduction. However, because reductions of lens gap junction proteins are central to the pathogenesis of cataracts in these mice and because 4-PBA treatment significantly increased fiber cell connexin levels, our data suggest that this kind of approach (perhaps using a combination of 4-PBA with other drugs) may have therapeutic potential.

Acknowledgments

This work was supported by National Institutes of Health Grant R01 EY08368 (ECB).

References

Ammerpohl O, Thormeyer D, Khan Z, Appelskog IB, Gojkovic Z, Almqvist PM, Ekstrom TJ, 2004 HDACi phenylbutyrate increases bystander killing of HSV-tk transfected glioma cells. Biochem. Biophys. Res. Commun 324, 8–14. [PubMed: 15464975]

Arora A, Minogue PJ, Liu X, Addison PK, Russel-Eggitt I, Webster AR, Hunt DM, Ebihara L, Beyer EC, Berthoud VM, Moore AT, 2008 A novel connexin50 mutation associated with congenital nuclear pulverulent cataracts. J. Med. Genet 45, 155–160. [PubMed: 18006672]

Basseri S, Lhotak S, Sharma AM, Austin RC, 2009 The chemical chaperone 4-phenylbutyrate inhibits adipogenesis by modulating the unfolded protein response. J. Lipid Res 50, 2486–2501. [PubMed: 19461119]

Batshaw ML, MacArthur RB, Tuchman M, 2001 Alternative pathway therapy for urea cycle disorders: twenty years later. J. Pediatr 138, S46–S54. [PubMed: 11148549]

Berthoud VM, Minogue PJ, Guo J, Williamson EK, Xu X, Ebihara L, Beyer EC, 2003 Loss of function and impaired degradation of a cataract-associated mutant connexin50. Eur. J. Cell Biol 82, 209–221. [PubMed: 12800976]

Berthoud VM, Minogue PJ, Lambert PA, Snabb JI, Beyer EC, 2016 The cataract-linked mutant Connexin50D47A causes endoplasmic reticulum stress in mouse lenses. J. Biol. Chem 291, 17569–17578. [PubMed: 27317663]

Berthoud VM, Minogue PJ, Yu H, Schroeder R, Snabb JI, Beyer EC, 2013 Connexin50D47A decreases levels of fiber cell connexins and impairs lens fiber cell differentiation. Invest. Ophthalmol. Vis. Sci 54, 7614–7622. [PubMed: 24204043]

Beyer EC, Ebihara L, Berthoud VM, 2013 Connexin mutants and cataracts. Front. Pharmacol 4, 43- doi: 10.3389/fphar.2013.00043. [PubMed: 23596416]

Bradford MM, 1976 A rapid and sensitive method for the quantitation of microgram quantities of protein using the principle of protein-dye binding. Anal. Biochem 72, 248–254. [PubMed: 942051]

Cheong N, Madesh M, Gonzales LW, Zhao M, Yu K, Ballard PL, Shuman H, 2006 Functional and trafficking defects in ATP binding cassette A3 mutants associated with respiratory distress syndrome. J. Biol. Chem 281, 9791–9800. [PubMed: 16415354]

Favor J, 1983 A comparison of the dominant cataract and recessive specific-locus mutation rates induced by treatment of male mice with ethylnitrosourea. Mutat. Res 110, 367–382. [PubMed: 6877261]

Gong B, Zhang LY, Lam DS, Pang CP, Yam GH, 2010 Sodium 4-phenylbutyrate ameliorates the effects of cataract-causing mutant gammaD-crystallin in cultured cells. Mol. Vis 16, 997–1003. [PubMed: 20577655]

Hayashi H, Sugiyama Y, 2007 4-phenylbutyrate enhances the cell surface expression and the transport capacity of wild-type and mutated bile salt export pumps. Hepatology 45, 1506–1516. [PubMed: 17538928]

Kemter E, Sklenak S, Rathkolb B, Hrabe de Angelis M, Wolf E, Aigner B, Wanke R, 2014 No amelioration of uromodulin maturation and trafficking defect by sodium 4-phenylbutyrate *in vivo*: studies in mouse models of uromodulin-associated kidney disease. J. Biol. Chem 289, 10715–10726. [PubMed: 24567330]

Kolb PS, Ayaub EA, Zhou W, Yum V, Dickhout JG, Ask K, 2015 The therapeutic effects of 4-phenylbutyric acid in maintaining proteostasis. Int. J. Biochem. Cell Biol 61, 45–52. [PubMed: 25660369]

Khan Z, Akhtar M, Asklund T, Juliusson B, Almqvist PM, Ekstrom TJ, 2007 HDAC inhibition amplifies gap junction communication in neural progenitors: potential for cell-mediated enzyme prodrug therapy. Exp. Cell Res 313, 2958–2967. [PubMed: 17555745]

Koyama M, Furuhashi M, Ishimura S, Mita T, Fuseya T, Okazaki Y, Yoshida H, Tsuchihashi K, Miura T, 2014 Reduction of endoplasmic reticulum stress by 4-phenylbutyric acid prevents the development of hypoxia-induced pulmonary arterial hypertension. Am. J. Physiol. Heart Circ. Physiol 306, H1314–H1323. [PubMed: 24610918]

Lam HC, Cloonan SM, Bhashyam AR, Haspel JA, Singh A, Sathirapongsasuti JF, Cervo M, Yao H, Chung AL, Mizumura K, An CH, Shan B, Franks JM, Haley KJ, Owen CA, Tesfaigzi Y, Washko GR, Quackenbush J, Silverman EK, Rahman I, Kim HP, Mahmood A, Biswal SS, Ryter SW, Choi AM, 2013 Histone deacetylase 6-mediated selective autophagy regulates COPD-associated cilia dysfunction. J. Clin. Invest 123, 5212–5230. [PubMed: 24200693]

Lee CS, Hanna AD, Wang H, Dagnino-Acosta A, Joshi AD, Knoblauch M, Xia Y, Georgiou DK, Xu J, Long C, Amano H, Reynolds C, Dong K, Martin JC, Lagor WR, Rodney GG, Sahin E, Sewry C, Hamilton SL, 2017 A chemical chaperone improves muscle function in mice with a RyR1 mutation. Nat. Commun 8, 14659. [PubMed: 28337975]

Makley LN, McMenimen KA, DeVree BT, Goldman JW, McGlasson BN, Rajagopal P, Dunyak BM, McQuade TJ, Thompson AD, Sunahara R, Klevit RE, Andley UP, Gestwicki JE, 2015 Pharmacological chaperone for alpha-crystallin partially restores transparency in cataract models. Science 350, 674–677. [PubMed: 26542570]

Minogue PJ, Tong JJ, Arora A, Russell-Eggitt I, Hunt DM, Moore AT, Ebihara L, Beyer EC, Berthoud VM, 2009 A mutant connexin50 with enhanced hemichannel function leads to cell death. Invest. Ophthalmol. Vis. Sci 50, 5837–5845. [PubMed: 19684000]

Mu TW, Ong DS, Wang YJ, Balch WE, Yates JR, III, Segatori L, Kelly JW, 2008 Chemical and biological approaches synergize to ameliorate protein-folding diseases. Cell 134, 769–781. [PubMed: 18775310]

Reddy MA, Francis PJ, Berry V, Bhattacharya SS, Moore AT, 2004 Molecular genetic basis of inherited cataract and associated phenotypes. Surv. Ophthalmol 49, 300–315. [PubMed: 15110667]

Rubenstein RC, Egan ME, Zeitlin PL, 1997 In vitro pharmacologic restoration of CFTR-mediated chloride transport with sodium 4-phenylbutyrate in cystic fibrosis epithelial cells containing delta F508-CFTR. J. Clin. Invest 100, 2457–2465. [PubMed: 9366560]

Shanmugam PM, Barigali A, Kadaskar J, Borgohain S, Mishra DK, Ramanjulu R, Minija CK, 2015 Effect of lanosterol on human cataract nucleus. Indian J. Ophthalmol 63, 888–890. [PubMed: 26862091]

Shiels A, Bennett TM, Hejtmancik JF, 2010 Cat-Map: putting cataract on the map. Mol. Vis 16, 2007–2015. [PubMed: 21042563]

Steele EC, Jr., Lyon MF, Favor J, Guillot PV, Boyd Y, Church RL, 1998 A mutation in the connexin 50 (Cx50) gene is a candidate for the No2 mouse cataract. Curr. Eye Res 17, 883–889. [PubMed: 9746435]

Teckman JH, 2004 Lack of effect of oral 4-phenylbutyrate on serum alpha-1-antitrypsin in patients with α−1-antitrypsin deficiency: a preliminary study. J. Pediatr. Gastroenterol. Nutr 39, 34–37. [PubMed: 15187777]

Upagupta C, Carlisle RE, Dickhout JG, 2017 Analysis of the potency of various low molecular weight chemical chaperones to prevent protein aggregation. Biochem. Biophys. Res. Commun 486, 163–170. [PubMed: 28285140]

Wang HZ, Rosati B, Gordon C, Valiunas V, McKinnon D, Cohen IS, Brink PR, 2015 Inhibition of histone deacetylase (HDAC) by 4-phenylbutyrate results in increased junctional conductance between rat corpora smooth muscle cells. Front. Pharmacol 6, 9. [PubMed: 25691868]

White TW, Goodenough DA, Paul DL, 1998 Targeted ablation of connexin50 in mice results in microphthalmia and zonular pulverulent cataracts. J. Cell Biol 143, 815–825. [PubMed: 9813099]

Xu X, Ebihara L, 1999 Characterization of a mouse Cx50 mutation associated with the No2 mouse cataract. Invest. Ophthalmol. Vis. Sci 40, 1844–1850. [PubMed: 10393059]

Yokoi N, Fukata Y, Kase D, Miyazaki T, Jaegle M, Ohkawa T, Takahashi N, Iwanari H, Mochizuki Y, Hamakubo T, Imoto K, Meijer D, Watanabe M, Fukata M, 2015 Chemical corrector treatment ameliorates increased seizure susceptibility in a mouse model of familial epilepsy. Nat. Med 21, 19–26. [PubMed: 25485908]

Zhao L, Chen XJ, Zhu J, Xi YB, Yang X, Hu LD, Ouyang H, Patel SH, Jin X, Lin D, Wu F, Flagg K, Cai H, Li G, Cao G, Lin Y, Chen D, Wen C, Chung C, Wang Y, Qiu A, Yeh E, Wang W, Hu X, Grob S, Abagyan R, Su Z, Tjondro HC, Zhao XJ, Luo H, Hou R, Jefferson J, Perry P, Gao W, Kozak I, Granet D, Li Y, Sun X, Wang J, Zhang L, Liu Y, Yan YB, Zhang K, 2015 Lanosterol reverses protein aggregation in cataracts. Nature 523, 607–611. [PubMed: 26200341]

Highlights

- The chemical chaperone 4-phenylbutyrate (4-PBA) is effective in some diseases caused by misfolded proteins.
- Mice expressing the connexin mutant, Cx50D47A, were treated with 4-PBA.
- Levels of Cx46 and Cx50 were improved in lenses of 4-PBA-treated mice.
- The distribution of Cx46 was improved in lenses of 4-PBA-treated mice.

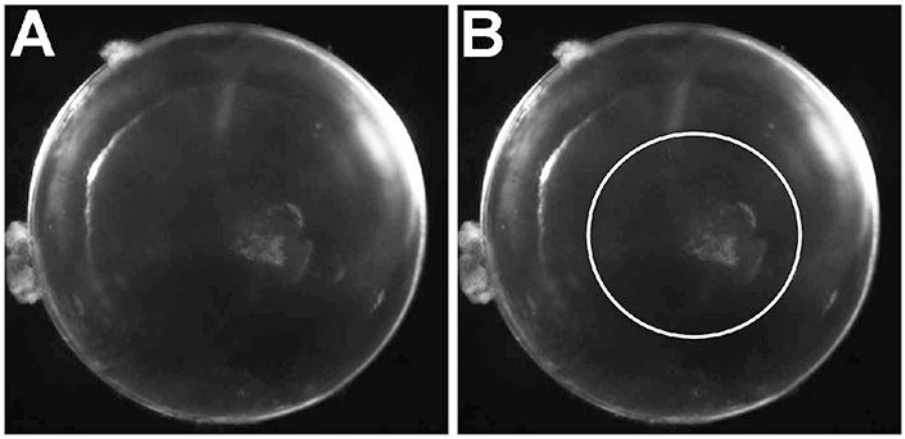

Figure 1.

Cataract quantification. A. Darkfield image of a mouse lens containing a small central cataract. B. Photomicrograph of the same lens showing the region of interest (interior of the white circle) used to quantify the opacity with the NIH ImageJ software. The size of the region of interest was selected so that it contained the opacity in the lens image with the biggest cataract. To quantify the opacity, the mean gray value within the region was multiplied by its area in pixels.

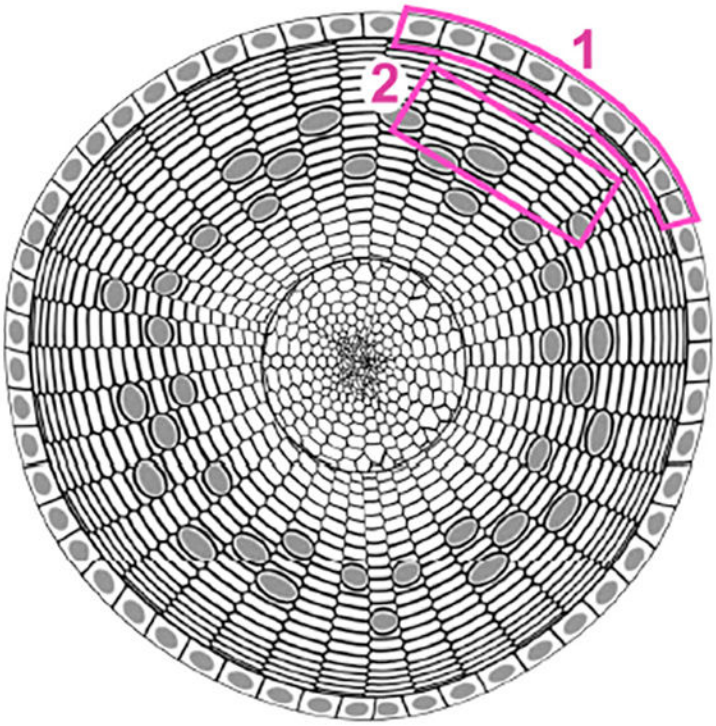

Figure 2.

Quantification of connexin immunostaining. Diagram of a cross section through a mouse lens illustrating the surface and fiber regions (areas 1 and 2, respectively, delimited by the pink lines) used to quantify the mean gray value and particles of connexin immunoreactivity (as described in Materials and Methods). Area 1 included epithelium and a small number of underlying fiber cells. Area 2 encompassed multiple layers of cortical fiber cells.

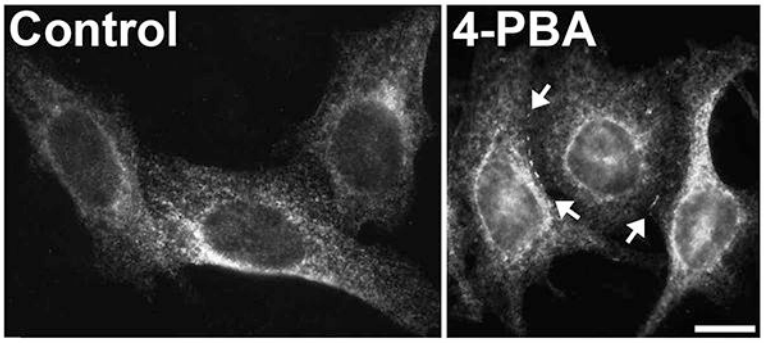

Figure 3.

4-PBA treatment rescues Cx50D47A trafficking and formation of gap junction plaques. Immunofluorescence micrographs show localization of Cx50D47A in HeLa cells transiently transfected with the mutant connexin and then left untreated (Control) or treated by addition of 4-PBA to the culture medium (4-PBA) for 24 hrs. Arrows indicate punctate staining at appositional membranes between cells, likely representing gap junction plaques. Bar, 16 μm.

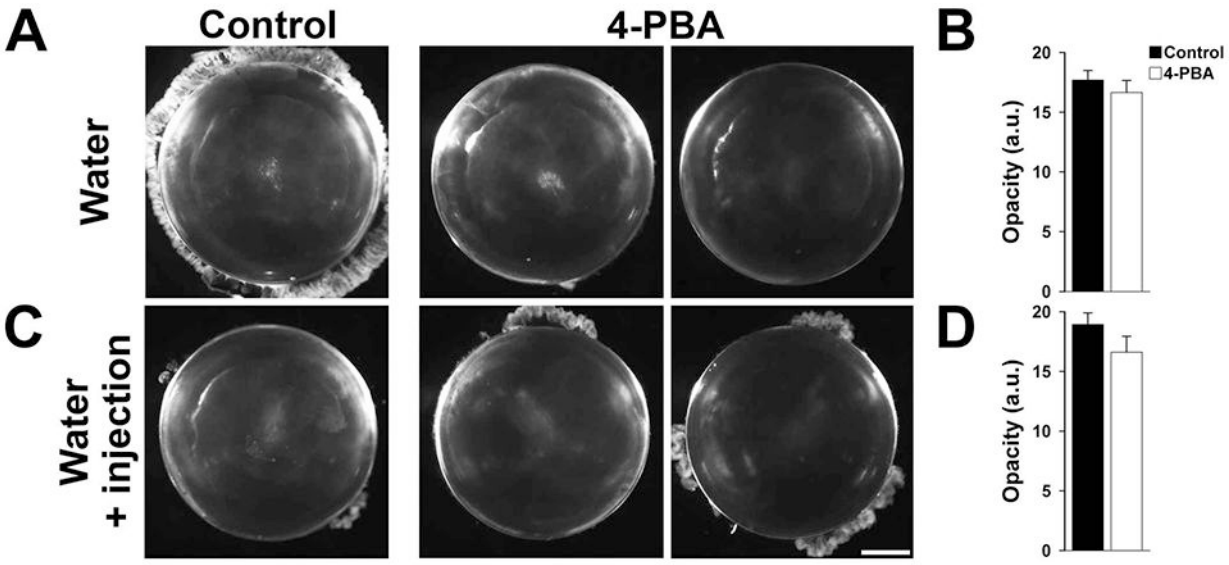

Figure 4.

Cataracts are present in both control and 4-PBA-treated lenses. A. Darkfield micrographs of lenses from a 1-month-old mouse that was untreated (Control) and from two different mice that were treated by addition of 4-PBA to the drinking water (4-PBA). C. Darkfield micrographs of lenses from a 1-month-old (Control) mouse that was injected with saline alone and from two different mice that were treated by addition of 4-PBA to the drinking water and parenteral injections (4-PBA). Bar, 410 μm. B, D. Graphs show the quantitation of the cataract (opacity) (n = 5 for Control and 4 for 4-PBA in B; n = 6 for Control and 4-PBA in D). The values did not show a significant difference between 4-PBA and Controls (for B, $p = 0.45$ and for D, $p = 0.19$.)

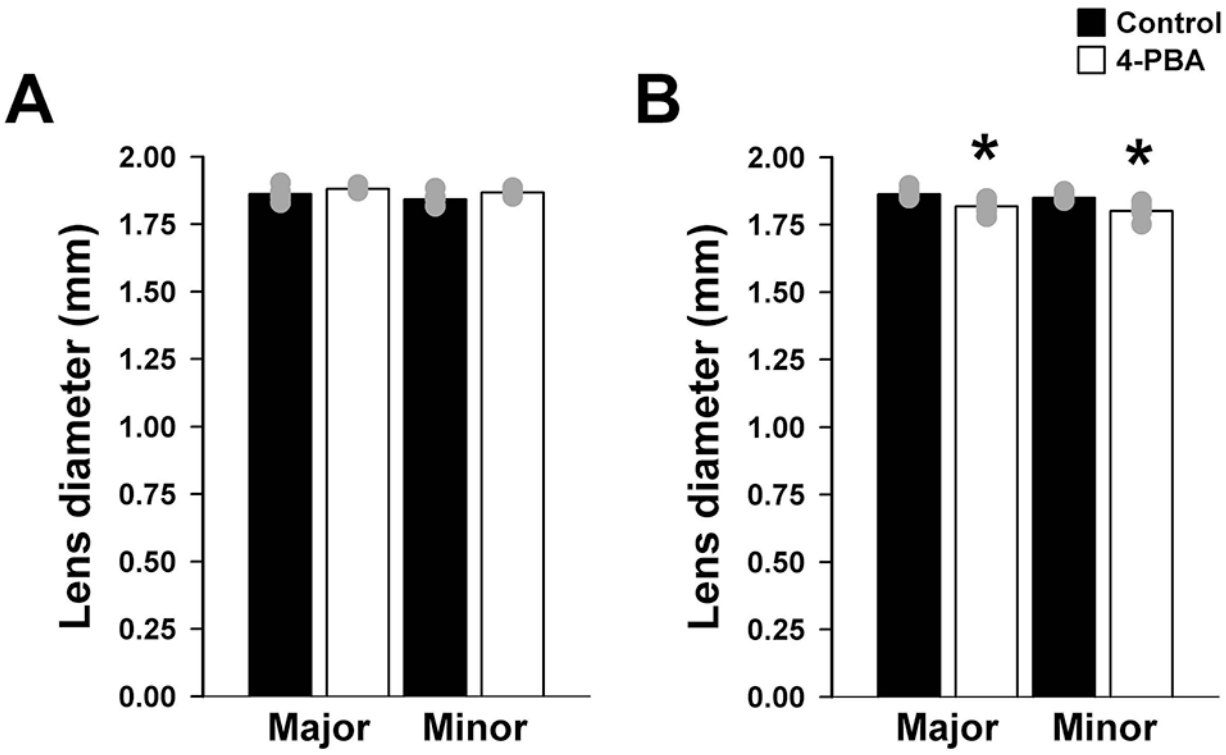

Figure 5.

Treatment with 4-PBA does not increase lens size. A, B. Graphs show the major and minor diameters determined from darkfield micrographs of lenses from mice that were untreated or were treated with 4-PBA by addition to the drinking water alone (A) or by addition to the drinking water and parenteral injections (B). Bars represent the mean of the individual values (gray circles) for each condition. *, $p < 0.01$. (For A, $p = 0.21$ for the major lens diameter and $p = 0.12$ for the minor lens diameter; for B, $p = 0.0045$ for the major lens diameter and $p = 0.0068$ for the minor lens diameter.)

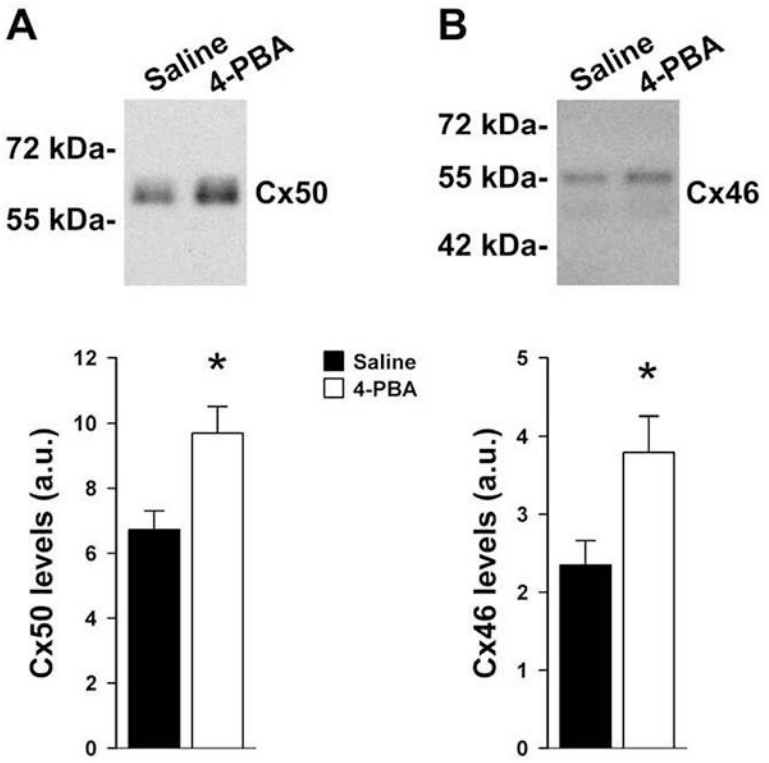

Figure 6.

4-PBA treatment increases levels of both lens fiber cell connexins. Top panels. Immunoblots of Cx50 (A) and Cx46 (B) in lens homogenates prepared from 1-month-old mice after treatment with 4-PBA by addition to the drinking water and injection (4-PBA) and from saline-injected controls (Saline). The migration positions of the molecular mass markers are indicated on the left. Bottom panels. Graphs show the quantitation (expressed in arbitrary units) of the immunoreactive bands obtained from blots of lenses from different animals (Cx50, n = 6 for saline- and 4-PBA-treated mice; Cx46, n = 5 for saline-treated mice and n = 6 for 4-PBA-treated mice). Data are presented as mean ± S.E.M. *, $p < 0.05$. (For Cx50, $p = 0.014$; for Cx46, $p = 0.031$.)

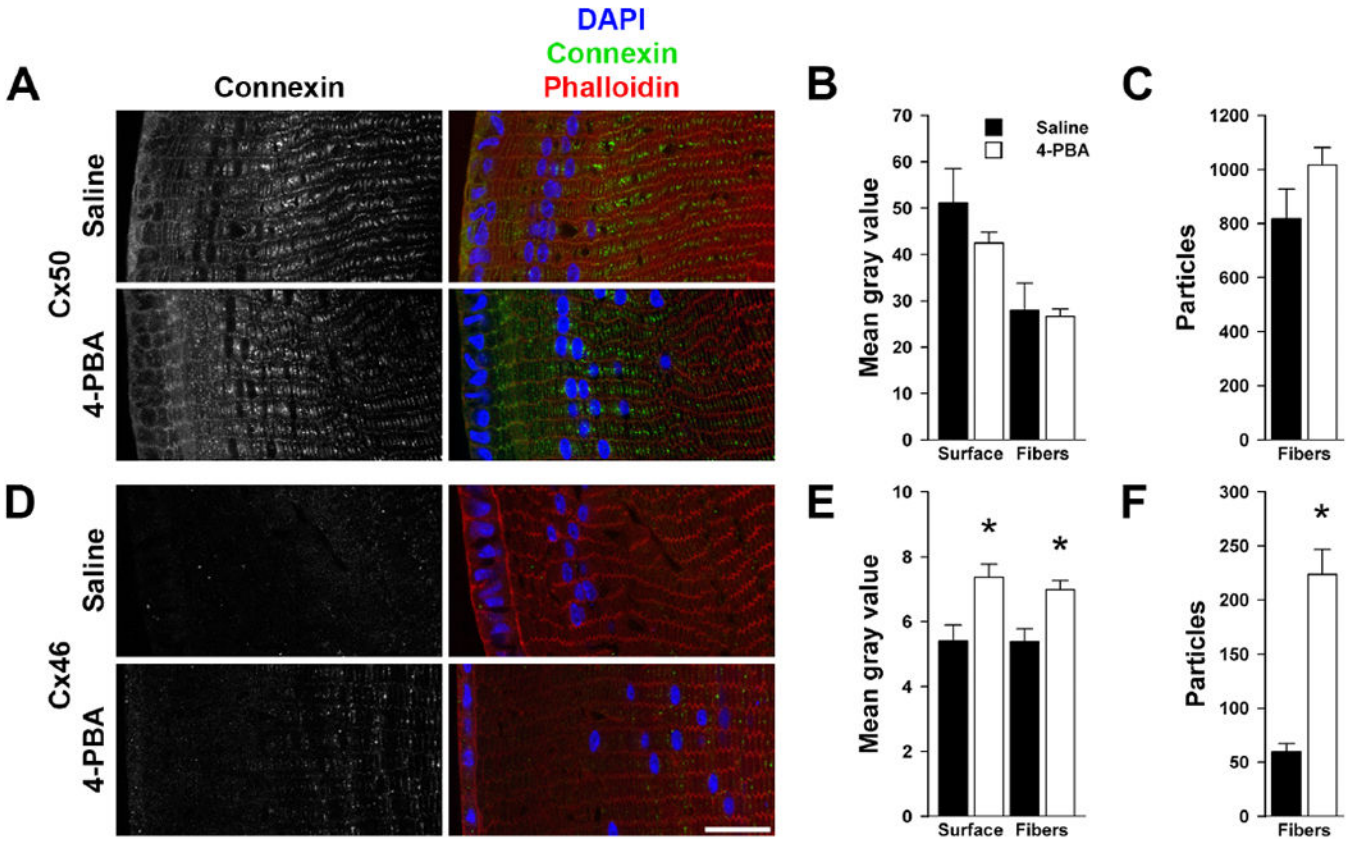

Figure 7.

4-PBA increases Cx46 immunoreactivity and puncta, but does not significantly affect Cx50 distribution. A, D. Confocal images show immunolocalization of Cx50 (A) and Cx46 (D) in sections of lenses from 1-month-old mice after treatment with 4-PBA by addition to the drinking water and injection (4-PBA) and from saline-injected controls (Saline). Left panels show localization of connexin immunoreactivity alone. Right panels show the superposition of connexin immunoreactivity (green) with DAPI-stained nuclei (blue) and filamentous actin (red) detected by phalloidin binding. Bar, 27 μm. B, E. Graphs show quantitation of mean gray values for Cx50 (B) and Cx46 (E) immunostaining in superficial (surface) and fiber cell regions (mean ± S.E.M.). C, F. Graphs show quantitation of the numbers of Cx50 (C) and Cx46 (F) immunoreactive particles within comparably-sized regions of interest (mean ± S.E.M.). *, $p < 0.05$. (For B surface, $p = 0.28$; for B fibers, $p = 0.84$; for C, $p = 0.14$; for E surface, $p = 0.0073$; for E fibers, $p = 0.036$; for F, $p = 3.52 \times 10^{-5}$.)

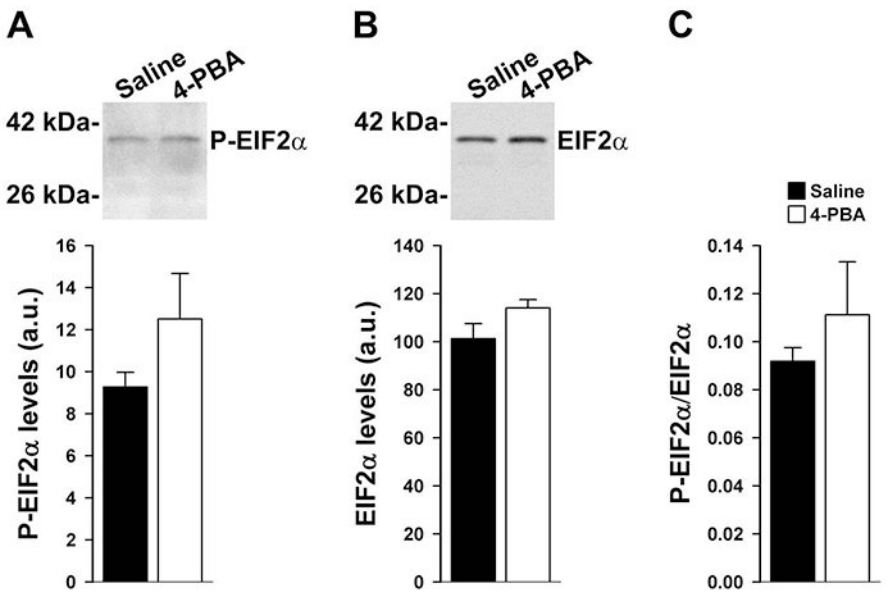

Figure 8.

4-PBA treatment does not decrease the activation of EIF2α. A, B (top panels). Immunoblots of phosphorylated EIF2a (P-EIF2α, A) and total EIF2α (EIF2a, B) performed on lens homogenates of 1-month-old mice following treatment with 4-PBA by addition to the drinking water and parenteral injection (4-PBA) and from saline-injected controls (Saline). The migration positions of the molecular mass markers are indicated on the left. A - C (bottom panels). Graphs show quantitation of P-EIF2α (A), total EIF2a (B), and the phosphorylated:total EIF2α ratio (P-EIF2α/EIF2α, C). Data are presented as mean (bar) ± S.E.M. (n = 4). (For A, p = 0.24; for B, p = 0.14; for C, p = 0.45.)

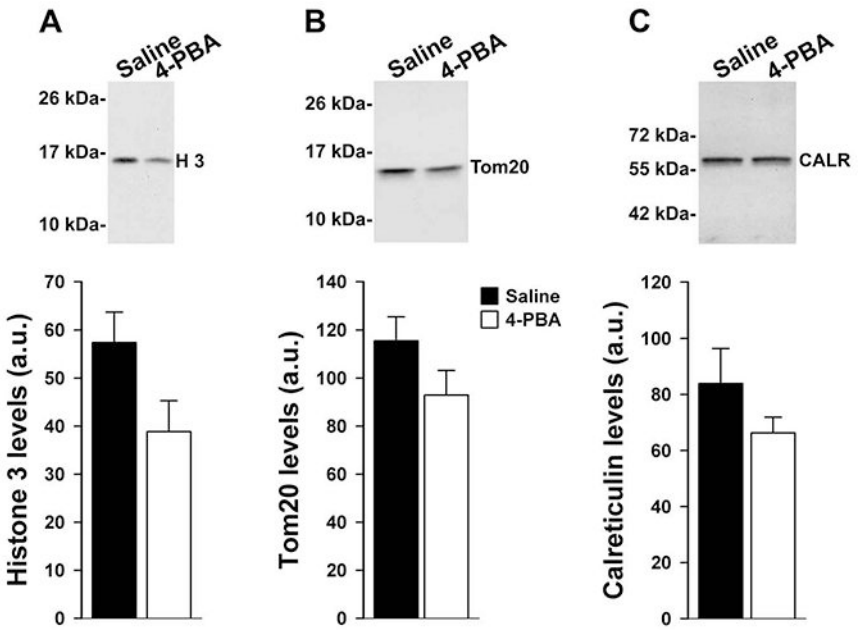

Figure 9.

4-PBA treatment has little or no effect on proteins from subcellular compartments that are increased in Cx50D47A mice. A - C (top panels). Immunoblots of histone 3, H 3 (A), Tom20 (B), and calreticulin, CALR (C) performed on lens homogenates of 1-month-old mice following treatment with 4-PBA by addition to the drinking water and parenteral injection (4-PBA) and from saline-injected controls (Saline). The migration positions of the molecular mass markers are indicated on the left. A - C (bottom panels). Graphs show quantitation of histone 3 (A), Tom20 (B), and calreticulin (C). Data are presented as mean (bar) ± S.E.M. (n = 6 for A; n = 4 for B and C). The values for treated mice were not significantly different from those of saline-injected controls with a cut-off of $p < 0.05$. (For A, $p = 0.065$; for B, $p = 0.16$; for C, $p = 0.27$.)